

OBSCURED AND UNOBSCURED ACTIVE GALACTIC NUCLEI IN THE SPITZER SPACE TELESCOPE FIRST LOOK SURVEY

M. LACY¹, L.J. STORRIE-LOMBARDI¹, A. SAJINA², P.N. APPLETON¹, L. ARMUS¹, S.C. CHAPMAN¹, P.I. CHOI¹, D. FADDA¹, F. FANG¹, D.T. FRAYER¹, I. HEINRICHSEN¹, G. HELOU¹, M. IM³, F.R. MARLEAU¹, F. MASCI¹, D.L. SHUPE¹, B.T. SOIFER¹, J. SURACE¹, H.I. TEPLITZ¹, G. WILSON¹, L. YAN¹

To appear in the ApJ Supp Spitzer special issue

ABSTRACT

Selection of active galactic nuclei (AGN) in the infrared allows the discovery of AGN whose optical emission is extinguished by dust. In this paper, we use the *Spitzer Space Telescope* First Look Survey (FLS) to assess what fraction of AGN with mid-infrared luminosities comparable to quasars are missed in optical quasar surveys due to dust obscuration. We begin by using the Sloan Digital Sky Survey (SDSS) database to identify 54 quasars within the 4 deg² extragalactic FLS. These quasars occupy a distinct region in mid-infrared color space by virtue of their strong, red, continua. This has allowed us to define a mid-infrared color criterion for selecting AGN candidates. About 2000 FLS objects have colors consistent with them being AGN, but most are much fainter in the mid-infrared than the SDSS quasars, which typically have 8 μ m flux densities, $S_{8.0}$, \sim 1mJy. We have investigated the properties of the 43 objects with $S_{8.0} \geq$ 1mJy satisfying our AGN color selection. This sample should contain both unobscured quasars, and AGN which are absent from the SDSS survey due to extinction in the optical. After removing 16 known quasars, three probable normal quasars, and eight spurious or confused objects from the initial sample of 43, we are left with 16 objects which are likely to be obscured quasars or luminous Seyfert-2 galaxies. This suggests the numbers of obscured and unobscured AGN are similar in samples selected in the mid-infrared at $S_{8.0} \sim$ 1mJy.

Subject headings: quasars:general – galaxies:Seyfert – infrared:galaxies

1. INTRODUCTION

The number of AGN missed in optical or soft X-ray surveys due to obscuring columns of dust and gas in the host is still an open question (e.g., Webster et al. 1995; Cutri et al. 2001; Gregg et al. 2003; Norman et al. 2002; Richards et al. 2003). Understanding and quantifying the population of obscured AGN is important if we are to obtain a complete picture of the build-up of black holes in the nuclei of galaxies. The close link between bulge mass and black hole mass (e.g. Magorrian et al. 1998) implies that understanding this history will also help us to understand the galaxy formation process as a whole.

The local mass density in black holes is dominated by the $\sim 10^{8.5} M_{\odot}$ black holes in L^* elliptical galaxies. When accreting at Eddington rates, these correspond to luminous quasars ($M_B \approx -25$). Recent work on the X-ray background, however, indicates that most of the mass build-up may occur on longer timescales at sub-Eddington rates, mostly in obscured AGN (Cowie et al. 2003). Besides X-ray searches, other techniques for finding obscured AGN have also been employed. A sample of luminous narrow-line AGN has been selected from the SDSS (Zakamska et al. 2003). Quasar samples selected in the near-infrared from the Two Micron All-Sky Survey (2MASS) (Cutri et al. 2001; Glikman et al. 2004) have identified a number of quasars with significant optical

extinction and X-ray columns. Even in the mid-infrared (MIR), a highly-obscured AGN will still have significant extinction. However, the disk or torus-like geometry of the obscuring material means that even if the extinction to the broad-line region is high, MIR light will usually be visible, unless the geometry is truly edge-on, or the AGN is completely enveloped in a dense cloud of dust and gas (Pier & Krolik 1993; Efsthathiou & Rowan-Robinson 1995). Thus an MIR survey can usefully address the question of the number of obscured AGN.

Studies with the *Infrared Space Observatory* (ISO) have shown that the strong MIR continuum associated with AGN provide a unique spectral signature that can be used to distinguish AGN from starbursts. The MIR continuum from galaxies arises mostly from three sources: HII regions dominated by emission from very small dust grains (producing a steeply-rising continuum at 12-16 μ m), photodissociation regions dominated by bands of Polycyclic Aromatic Hydrocarbon (PAH) emission, and AGN dominated by a strong 3-10 μ m continuum. Laurent et al. (2000) show that the spectral energy distributions (SEDs) arising from each of these is sufficiently distinct to allow discrimination of AGN from star-forming galaxies based on their MIR SEDs. Using these ideas, Haas et al. (2004) combined near- and mid-infrared colors to select AGN from an ISO parallel survey. With the advent of *Spitzer* (Werner et al. 2004) it has become possible to obtain MIR photometry for large samples of field galaxies, and thus to use the MIR SEDs to identify specific populations of AGN and star-forming galaxies. In this paper we use SDSS quasars to provide an empirical localization of the AGN population in mid-infrared color space. We then select a sample of candidate obscured AGN with 8 μ m flux densities ($S_{8.0}$)

¹ Spitzer Science Center, Caltech, MS 220-6, Pasadena, CA 91125; mlacy,lisa@ipac.caltech.edu

² Department of Physics & Astronomy, University of British Columbia, 6224 Agricultural Road, Vancouver, BC V6T1Z1, Canada, sajina@astro.ubc.ca

³ Astronomy Program, School of Earth and Environmental Sciences, Seoul National University, Shillim-dong, Kwanak-gu, Seoul, S. Korea 2-880-9010

$\geq 1\text{mJy}$, and compare their optical identifications and estimated redshifts to those of the SDSS quasars with $S_{8.0} \geq 1\text{mJy}$. We use the main field of the extragalactic component of the *Spitzer* First Look Survey (FLS), a shallow, 4 deg^2 survey with the Infrared Array Camera (IRAC; Fazio et al. 2004) and the Multiband Imaging Photometer for *Spitzer* (MIPS; Rieke et al. 2004), for which an extensive multiwavelength ancillary dataset exists. We assume a cosmology with $\Omega_M = 0.3$, $\Omega_\Lambda = 0.7$ and $H_0 = 70\text{kms}^{-1}\text{Mpc}^{-1}$.

2. THE SPITZER FLS MAIN FIELD DATASET

The FLS observations were made in December 2003 (program ID 26, astronomical observation request (AOR) IDs 3861504, 3861760, 3862016, 3862016, 3862272, 3862528, 3862784, 3863040, 3863296, 3863552). We have used preliminary versions of the IRAC catalog (Lacy et al. 2004) and the MIPS $24\mu\text{m}$ catalog (Fadda et al. 2004b). The IRAC catalog has flux density limits (5σ in a $5''$ diameter aperture) in the four IRAC channels with nominal central wavelengths of $3.6\mu\text{m}$, $4.5\mu\text{m}$, $5.8\mu\text{m}$ and $8.0\mu\text{m}$, of $S_{3.6} \approx 7\mu\text{Jy}$, $S_{4.5} \approx 8\mu\text{Jy}$, $S_{5.8} \approx 60\mu\text{Jy}$, and $S_{8.0} \approx 50\mu\text{Jy}$. The MIPS $24\mu\text{m}$ catalog has a flux density limit of $\approx 300\mu\text{Jy}$.

3. THE SDSS QUASARS

The Sloan Data Release 1 (DR1) quasar survey (Schneider et al. 2003) contains 54 quasars which fall within the main field of the FLS. All are detected with IRAC, and all but one at $24\mu\text{m}$ with MIPS. Three more quasars were found as a result of spectroscopic follow-up of the radio survey of Condon et al. (2003) using the Kast Spectrograph at Lick Observatory.

4. THE POSITION OF SDSS QUASARS IN MIR COLOR-COLOR PLOTS

An IRAC color-color plot, using all four broad-band channels of the IRAC instrument, is shown in Figure 1. The dots indicate the location of ≈ 16000 objects in the main field catalog. Plotting the $8.0\mu\text{m}/4.5\mu\text{m}$ ratio against the $5.8\mu\text{m}/3.6\mu\text{m}$ ratio makes the color-color plot effective at separating objects with blue continua from those with red. Most objects have blue colors in both axes. These are most likely stars, or low-redshift galaxies whose SEDs are weak in non-stellar light, e.g., elliptical galaxies. From this clump two distinct “sequences” can be seen. One has blue colors in $S_{5.8}/S_{3.6}$ and very red colors in $S_{8.0}/S_{4.5}$. These are most likely low-redshift ($z \lesssim 0.2$) galaxies with the centers of their 6.2 and $7.7\mu\text{m}$ PAH emission bands (Puget & Léger 1989) redshifted into the IRAC $8.0\mu\text{m}$ filter. The other sequence has red colors in both pairs of filters and it is on this sequence that the SDSS and radio-selected quasars lie. Note that strong stellar light will shift the $S_{5.8}/S_{3.6}$ ratio to the blue, as illustrated by the two filled squares in Figure 1. These objects are classed as quasars in the SDSS database, but have resolved host galaxies in the IRAC images, and so are classed as Seyfert-1s in this study.

5. MIR SELECTION OF CANDIDATE AGN

We used *Spitzer* colors of the SDSS quasars to empirically define a color selection which will pick out objects with MIR SEDs consistent with their being AGN. This is the region enclosed by the dashed line in Figure 1. Our

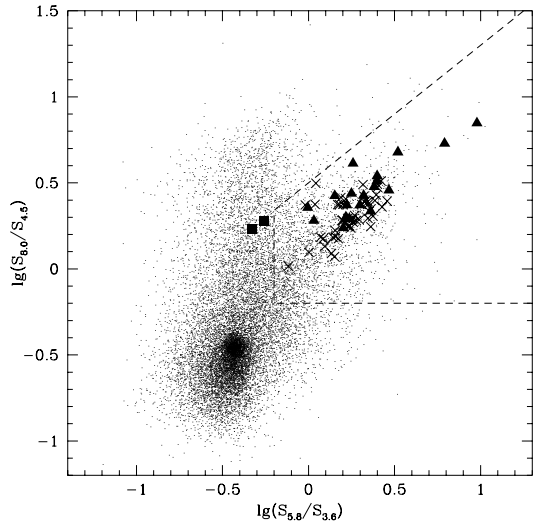


FIG. 1.— An IRAC color-color plot using the main field FLS data. Dots represent the ≈ 16000 objects with “clean” detections in all four IRAC bands. Crosses indicate the colors of all the SDSS and radio-selected quasars, squares the SDSS Seyfert 1 galaxies and triangles the bright ($S_{8\mu\text{m}} \geq 1\text{mJy}$) sample of obscured AGN. The dashed line shows the color criteria used to pick out the AGN sample.

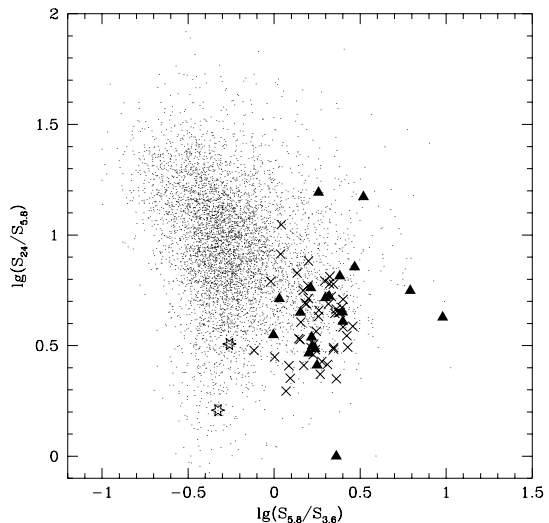


FIG. 2.— An IRAC-MIPS $24\mu\text{m}$ color-color plot. Dots represent objects with “clean” detections in all four IRAC bands matched to the MIPS $24\mu\text{m}$ catalog of Fadda et al. (2004b), totalling ≈ 6000 objects. Crosses indicate the colors of SDSS quasars, stars the SDSS Seyfert 1 galaxies and triangles the $S_{8.0} \geq 1\text{mJy}$ sample of obscured AGN candidates.

modelling of MIR SEDs based on *ISO* spectra (Sajina, Lacy & Scott 2004) suggests that most of the objects in this region are indeed dominated by AGN emission, though we expect some contamination by star-forming galaxies close to the boundaries. There are ≈ 2000 sources in this region, which are therefore likely to contain AGN. Most of them are fainter in the MIR than the SDSS quasars, which are typically much brighter than the FLS flux density limits.

To pick a sample of AGN selected in the MIR which we

could compare directly to the SDSS quasar sample, we examined the distribution of $S_{8.0}$ for the SDSS sample. ($8.0\mu\text{m}$ is the longest IRAC wavelength, and therefore least affected by dust obscuration.) This distribution showed a peak at $S_{8.0} \approx 1\text{mJy}$, and we therefore assumed that at $S_{8.0} \geq 1\text{mJy}$ most of our MIR-selected AGN would appear in the SDSS sample if they were not obscured by dust.

There are 43 objects within the AGN selection region of the color-color plot with $S_{8.0} \geq 1\text{mJy}$ and “clean” detections in the IRAC FLS catalogue [i.e. unblended (about 80% of the 4-band detections), and outside the haloes of bright stars and unaffected by multiplexer bleed or pulldown (97.6% of the survey area)]. The steps used to determine which of these were candidate obscured AGN were as follows: (1) we matched the sample of 43 bright AGN candidates to the SDSS quasar list, finding that 14 of our 43 objects are known SDSS quasars; (2) we next matched to our list of radio-selected quasars, finding two objects in common; (3) we examined the objects by eye on the FLS mosaics, and rejected a further seven objects from the sample on the basis of them being either saturated stars, or confused in the IRAC images. This left 20 objects in the sample, which are our bright, obscured AGN candidates. These are shown as triangles in Figure 1, and listed in Table 1. As a check on the AGN nature of these candidates, in Figure 2 we plot a color-color plot which extends the wavelength range to MIPS $24\mu\text{m}$. The large wavelength difference between 8 and $24\mu\text{m}$ makes the interpretation of the MIPS/IRAC color-color plots more complicated, but it can be seen that most of the obscured AGN candidates lie in the same region of the plot as the SDSS quasars, consistent with them having SEDs dominated by emission from hot dust around the AGN. Starburst galaxies typically have much redder $S_{24}/S_{5.8}$ colors due to a lack of high temperature dust emission from the AGN.

All our 20 bright, obscured AGN candidates (and all the SDSS quasars) were identified on the R -band images of Fadda et al. (2004a) (limiting $R \approx 25.5$). These identifications allowed us to further refine our selection. Out of the 20 obscured AGN candidates, we found that three had the MIR to optical color and stellar morphology of normal quasars (one apparently behind a spiral disk), one candidate is very bright ($R = 15.7$), so is probably either a peculiar star, or a foreground star within $\sim 1''$ of a background AGN. Of the remaining 16 objects, 14 are extended in R -band, and thus most likely galaxies whose AGN is completely obscured in the optical. Two are faint in R , but point-like and so are probably only partly obscured AGN. Figure 3 shows a plot of the ratio of R -band flux density ($S_{0.65}$) to $S_{8.0}$ plotted against $\lg(S_{8.0})$ for all 20 objects.

6. PHOTOMETRIC REDSHIFTS OF THE CANDIDATE AGN POPULATION

Of the 14 extended (galaxy) detections in R -band, 12 are detected on the SDSS DR1 images (which are significantly deeper than the SDSS spectroscopic quasar and galaxy surveys), and we have used their $ugri$ magnitudes to make a rough photometric redshift estimates using *Hyperz* (Bolzonella, Miralles & Pelló 2000), with the Bruzual & Charlot (1993) templates. (We exclude the z -band due to the likelihood of contamination by AGN

TABLE 1
CANDIDATE AGN NOT IN SDSS DR1 WITH $S_{8.0} \geq 1\text{mJy}$

Name	$S_{8.0}^1$ (mJy)	R	$S_{1.4\text{GHz}}^2$ (mJy)	z_{phot}^3	Opt Type ⁴
SSTXFLS J171106.8+590436	1.28	19.8	0.31	0.460	galaxy
SSTXFLS J171115.2+594906	4.53	21.0	0.12	-	stellar
SSTXFLS J171133.4+584055	1.91	18.6	0.09	-	see note (5)
SSTXFLS J171147.4+585839	1.56	21.0	0.57	(0.5)	galaxy
SSTXFLS J171313.9+603146	4.30	18.3	<0.09	0.155	galaxy
SSTXFLS J171324.3+585549	1.09	20.7	<0.09	0.635	galaxy
SSTXFLS J171325.1+590531	1.19	18.3	0.16	0.105	galaxy
SSTXFLS J171421.3+602239	1.25	18.6	0.16	0.195	galaxy
SSTXFLS J171430.7+584225	1.85	19.9	0.16	0.135	galaxy
SSTXFLS J171708.6+591341	1.32	21.1	<0.09	0.195	galaxy
SSTXFLS J171804.6+602705	1.05	21.7	<0.09	(0.6)	galaxy
SSTXFLS J171831.6+595317	1.10	20.6	2.22	0.295	galaxy
SSTXFLS J171930.9+594751	1.44	19.6	0.56	0.355	galaxy
SSTXFLS J172050.4+591511	3.35	21.6	1.75	0.440	galaxy
SSTXFLS J172123.1+601214	3.40	18.8	0.26	0.355	galaxy
SSTXFLS J172253.9+582955	1.00	18.5	<0.09	-	stellar
SSTXFLS J172328.4+592947	1.48	22.2	0.31	-	stellar
SSTXFLS J172432.8+592646	3.04	15.7	<0.09	-	stellar ⁶
SSTXFLS J172458.3+591545	1.10	20.0	0.46	0.640	galaxy
SSTXFLS J172601.8+601100	1.43	20.3	<0.09	-	stellar

Notes: (1) preliminary flux densities only, errors $\approx 20\%$; (2) flux densities at 1.4GHz in the survey of Condon et al. (2003); (3) photometric redshifts, z_{phot} , those in brackets are obtained by assuming a galaxy luminosity of L^* , others are from *Hyperz* using the SDSS $ugri$ magnitudes; (4) optical classification in the R -band image; (5) this is a stellar object within the isophotes of a spiral disk, we assume it is a background quasar which happens to be behind a disk galaxy; (6) this object may be a star, see text.

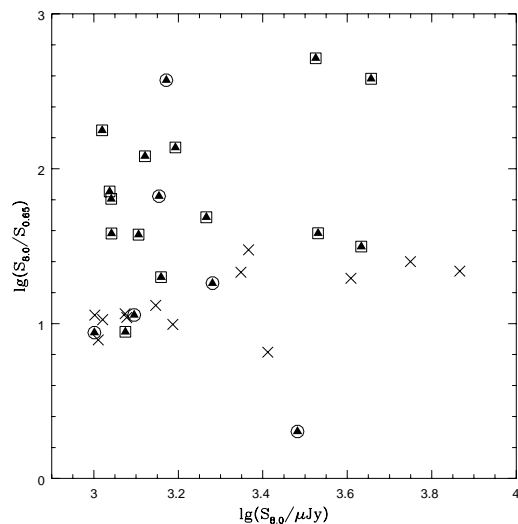


FIG. 3.— $S_{8.0}$ to R -band flux ratio as a function of $S_{8.0}$. SDSS quasars are shown as crosses, point-like identifications of AGN candidates are shown as triangles within circles, and triangles within squares denote galaxy identifications.

emission, but believe the other bands should be largely free of significant contamination given the extended appearance of the galaxies in the R -band data). The galaxies have a mean luminosity of $\approx L^*$, and inspection of the R -band image shows they appear to be mostly early-type galaxies. Our photometric redshifts are only approximate, but the magnitudes of the galaxies are such that few are likely to be at $z \gtrsim 0.7$.

7. DISCUSSION

Although we emphasize that the candidate obscured AGN we have identified from their MIR colors require spectroscopic confirmation as AGN, our study suggests that about 50% of AGN selected in the MIR at these flux levels may be sufficiently obscured by dust in the optical for them to be missed from the SDSS quasar survey. This excludes AGN which are not energetically dominant in their host galaxies (which would plot elsewhere on the IRAC color-color diagram), and any AGN which remain obscured in the MIR.

The median photometric redshift of our candidate obscured AGN is ≈ 0.36 (assuming the faint identifications with stellar morphologies to lie at high redshift), compared to ≈ 0.69 for the SDSS quasars with $S_{8.0} \geq 1\text{mJy}$. There is thus a hint that the obscured AGN may have lower redshifts and luminosities. Selection effects are unlikely to account for this difference. MIR selection ensures that the AGN are selected independent of their optical properties. Whilst we might be biased towards objects with more dust close to the AGN, this would not introduce a redshift bias if the fraction of such objects was constant with both luminosity and redshift. A lower median luminosity for the obscured AGN would, however, be consistent with the “receding torus” model (Lawrence 1991) in which a higher fraction of low-luminosity AGN are obscured, and might also be consistent with some studies of the X-ray background which find large numbers of low luminosity, relatively low redshift obscured AGN (Gilli et al. 2001; Gandhi & Fabian 2003; Steffen

et al. 2003).

If unobscured, our AGN would be moderately luminous, with B -band absolute magnitudes, $M_B, \approx -22$, on the boundary between Seyfert-1 galaxies and quasars. The brightest, $z \sim 0.6$, objects would have $M_B \sim -23$, in the quasar regime, and close to the median luminosity of the SDSS sample. Pursuing this work to lower $8\mu\text{m}$ flux densities, and using spectroscopy to confirm the AGN nature and redshift distribution of our objects, will help us link the infrared to the X-ray studies. This will allow us to derive a consistent story for the nature and evolution of obscured AGN, and thus for how and when the supermassive black holes in galaxies today accreted most of their mass.

We thank Michael Gregg for assistance with the Lick observations, Susan Ridgway for advice and comments, B. Januzzi and A. Ford for the R -band survey, and J. Condon for the VLA survey. We thank the SDSS team for targeting the FLS region in the DR1. This work is based on observations made with the *Spitzer Space Telescope*, operated by the Jet Propulsion Laboratory (JPL), California Institute of Technology under NASA contract 1407. Support was provided by NASA through JPL. The SDSS Archive is funded by the Alfred P. Sloan Foundation, the Participating Institutions, NASA, the National Science Foundation, the U.S. Department of Energy, the Japanese Monbukagakusho, and the Max Planck Society.

REFERENCES

- Bolzoniella, M., Miralles, J.-M. & Pelló, R. 2000, *A&A*, 363, 476
 Bruzual, G. & Charlot, S. 1993, *ApJ* 405, 538
 Condon, J.J., Cotton, W.D., Yin, Q.F., Shupe, D.L., Storrie-Lombardi, L.J., Helou, G., Soifer, B.T. & Werner, M.W. 2003, *AJ*, 125, 2411
 Cowie, L.L., Barger, A.J., Bautz, M.W., Brandt, W.N. & Garmire, G.P. 2003, *ApJ*, 584, L57
 Cutri, R.M., Nelson, B.O., Kirkpatrick, J.D., Huchra, J.P. & Smith, P.S. 2001, in *ASP Conf. Ser. 232, The New Era of Wide Field Astronomy*, ed. R. Clowes, A. Adamson, & G. Bromage (San Francisco: ASP), 78
 Efstathiou, A. & Rowan-Robinson, M. 1995, *MNRAS*, 273, 649
 Fadda, D., Januzzi, B., Ford, A. & Storrie-Lombardi, L.J. 2004a, *AJ*, in press (astro-ph/0403490)
 Fadda, D. et al. 2004b, in preparation
 Fazio, G. G. et al. 2004, *ApJS*, this volume.
 Gandhi, P. & Fabian, A.C. 2003, *MNRAS*, 339, 1095
 Gilli, R., Salvati, M. & Hasinger, G. 2001, *A&A* 366, 407
 Glikman, E., Gregg, M.D., Lacy, M., Helfand, D.J., Becker, R.H. & White, R.L. 2004, *ApJ*, in press (astro-ph/0402386)
 Gregg, M.D., Lacy, M., White, R.L., Glikman, E., Helfand, D., Becker, R.H. & Brotherton, M.S. 2002, *ApJ*, 563, 133
 Haas, M., Siebenmorgen, R., Leipski, C., Meusinger, H., Müller, S.A.H., Chini, R. & Schartel, N. 2004, *A&A*, in press (astro-ph/0404306)
 Lacy, M. et al. 2004, in preparation
 Laurent, O., Mirabel, I.F., Charmandaris, V., Gallais, P., Madden, S.C., Sauvage, M., Vigroux, L. & Cesarsky, C. 2000, *A&A*, 359, 887
 Lawrence, A. 1991, *MNRAS*, 252, 586
 Magorrian, J. et al. 1998, *AJ*, 115, 2285
 Norman, C. 2002, *ApJ*, 571, 218
 Pier, E.A. & Krolik, J.H. 1993, *ApJ*, 418, 673
 Puget, J.-L. & Léger, A. 1989, *Ann. Rev. A. Ap.* 27, 161
 Richards, G.T. et al. 2003, *AJ*, 126, 1131
 Rieke, G. H. et al. 2004, *ApJS*, this volume.
 Sajina, A., Lacy, M. & Scott, D. 2004, in preparation
 Schneider, D.P. et al. 2003, *AJ*, 126, 2579
 Steffen, A.T., Barger, A.J., Cowie, L.L., Mushotzky, R.F. & Yang, T. 2003, *ApJ*, 596, L23
 Webster, R.L., Francis, P.J., Peterson, B.A., Drinkwater, M.J., Masci, F.J. 1995, *Nature*, 375, 469
 Werner, M. et al. 2004, *ApJS*, this volume
 Zakamska, N.L. et al. 2003, *AJ*, 126, 2125